X-RAY STRUCTURAL ANALYSIS OF DUCTILE IRON WITH THE ADDITION OF NI HEAT-TREATED UNDER ISOTHERMAL CONDITIONS

OLEJARCZYK-WOŻEŃSKA Izabela[1], GIĘTKA Tomasz[2], ADRIAN Henryk[1], MRZYGŁÓD Barbara[1], GŁOWACKI Mirosław[1], GOŁY Marcin[1]

[1] AGH University of Science and Technology, Faculty of Metals Engineering and Industrial Computer Science, Cracow, Poland, EU, iolejarc@agh.edu.pl
[2] UTP University of Science and Technology, Faculty of Mechanical Engineering, Bydgoszcz, Poland, EU

Abstract

The results of the X-ray diffraction analysis of the pearlitic - ferritic ductile iron with the addition of Ni are presented. The cast iron was heat treated by austenitizing with the following austempering carried out under different conditions. Investigations covered the crystal structure parameters as well as the volume fractions of both austenite and ferrite. The effect of heat treatment parameters, i.e. of the time and temperature of austempering, on the austenite volume fraction and carbon content in this constituent was investigated.

Keywords: Ductile iron, austempered ductile iron (ADI), X-ray diffraction

1. INTRODUCTION

Austempered Ductile Iron (ADI) is the ductile iron with a ferritic - austenitic matrix structure, characterized by a preferred combination of high strength, ductility and fracture toughness. The wide range of ADI mechanical properties is obtained by properly adjusted heat treatment leading to the formation of final microstructure, which is a mixture of stable austenite and ferrite plates in the shape of "needles" (ausferrite). The type of the obtained structure is strongly influenced by the chemical composition of base ductile iron and heat treatment parameters, including austenitizing in the temperature range of 800-950 °C and austempering in the temperature range of 230-400 °C [1-4]. Properly selected time and temperature of austempering decide about the austenite content in cast iron matrix (5-40 %), while matrix microstructure shapes the mechanical properties. One of the methods for qualitative and quantitative evaluation of the matrix microstructure is the X-ray diffraction analysis. Applied to ADI, the X-ray diffraction is a fine tool to study the structure and distinguish between individual phases, i.e. between ferrite and austenite [5-8]. Compared with microscopic examinations, the diffraction studies cover a larger area [5, 9]. The technique adopted most often is a direct comparison with the reference concentrations and intensities of different compounds compiled in tables. The selected line of identification should always fall on the lines with the strongest intensity [10-12].

In this paper, the effect of austempering parameters on the volume fraction of metal matrix in ADI with the addition of Ni was discussed. The analysis covered a relationship between the austempering time and temperature and the volume fraction of austenite, carbon content in austenite and the length and size of the austenite and ferrite grains.

2. TEST MATERIAL AND METHODOLOGY

2.1. Test material

The X-ray diffraction studies were performed on polished samples used in the impact tests. The starting material was ductile iron with the chemical composition given in **Table 1**.

Table 1 Chemical composition of ductile iron

Chemical composition, wt. %						
C	**Si**	**Mn**	**Mg**	**Ni**	**P**	**S**
3.55	2.55	0.31	0.063	1.56	0.025	0.009

Melting was conducted according to ASTM A890 at the Foundry Research Institute in Cracow. Specimens for impact testing were cut out from the lower part of the keel block and were next subjected to the austempering treatment. Austempering was conducted in two temperature ranges, i.e. in the upper range and in the lower range. Austempering in the upper range was carried out for the time of t_{pi} = 90 minutes, and for the time of t_{pi} = 120 minutes in the lower range. The designations of individual heat treatment variants for the specific times and temperatures are shown in **Table 2**, while the schematic diagram of austempering is presented in **Figure 1**.

Table 2 Variants of the austempering treatment

Variant	T_{pi}, ℃	τ_{pi}, min
W12	400	90
W10	380	90
W8	360	90
W6	330	120
W4	300	120
W2	260	120

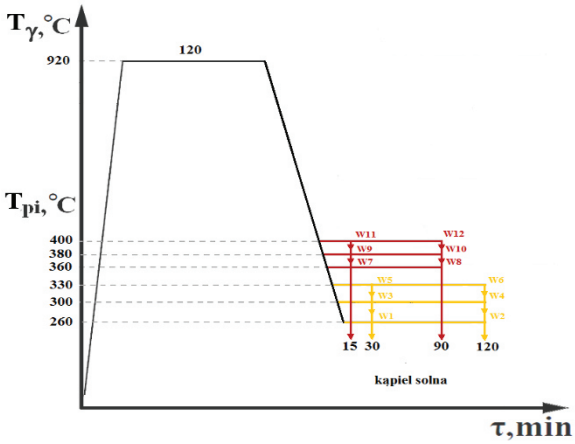

Figure 1 Schematic representation of the austempering treatment

2.2. X-ray structural analysis

The X-ray structural analysis was carried out using a DRON-1.5 diffractometer with iron-filtered CoK$_\alpha$ radiation. The following parameters of the diffractometer operation were adopted: tube voltage of 35 kV, tube excitation current of 8 mA, collimating ports in I-2, II-2, III-2 mm arrangement, Soller slits on primary and diffracted beam, scintillation counter detector supplied with voltage of 700 V. Recording of diffraction patterns was done in an angular range of 2Θ - 40.00÷68.00. Within this angular range, using a step of 0.04, the diffraction lines (110 and 200) of α phase and (111 and 200) of the γ phase were recorded.

The volume content of austenite (V_γ) in the matrix of austempered ductile iron was determined from equation (1) [13, 14, 7]:

$$V_\gamma = \frac{1}{1 + I_\alpha \cdot I_\gamma^{-1} \cdot R} \cdot 100\% \quad (1)$$

where: V_γ - volume fraction of austenite,%, I_α - total relative intensity of the diffraction line (110) of the α phase planimetered on the X-ray diffraction pattern, imp, I_γ^{-1} - total relative intensity of the diffraction line (111) of the γ phase planimetered on the X-ray diffraction pattern, imp, R - constant taken from [13]; for these measurements its value was 0.85.

The lattice constants for the γ and α phases were determined from equation (2) [13]:

$$a = \frac{\lambda}{2sin\Theta}\sqrt{h^2 + k^2 + l^2} \quad (2)$$

where: a - crystal lattice parameter, nm, λ - wavelength, nm, Θ - angle of diffraction determined from the diffraction pattern, °, *h, k, l* - Miller indices for the α and γ phases.

The concentration of carbon in austenite was determined from equation (3) [13]:

$$C_\gamma = \frac{a_\gamma - a_{Fe\gamma}}{0.0033} \quad 3)$$

where: C_γ - carbon content, wt %, a_γ - lattice parameter of austenite, nm, $a_{Fe\gamma}$ - lattice parameter of γ-phase iron - 0.3573 nm (the value extrapolated up to a temperature of 20 ℃).

From the set of X-ray patterns, the half-width values of the α phase ($b_{1/2\alpha}$) and of the γ phase ($b_{1/2\gamma}$) were determined and were next used for the calculation of an average size of the austenite and ferrite grains based on equation (4) [14]:

$$D = \frac{\Phi\lambda}{cos\theta\sqrt{b^2 - \left(\frac{\Delta a}{a}\right)^2 tg^2\theta}} \quad 4)$$

where: Φ - grain shape factor close to unity, λ - wavelength, nm, Θ - angle of the interference line determined from the diffraction pattern, °, b - total width of the diffraction line determined from the diffraction pattern, a - crystal lattice parameter, nm, Δa - the difference in lattice parameters, nm.

3. RESULTS AND DISCUSSION

The representative microstructures and selected X-ray diffraction patterns of specimens austempered at two isothermal temperatures are shown in **Figure 2**. The microstructure is fully ausferritic and consists of a mixture of ausferritic ferrite and carbon-enriched retained austenite.

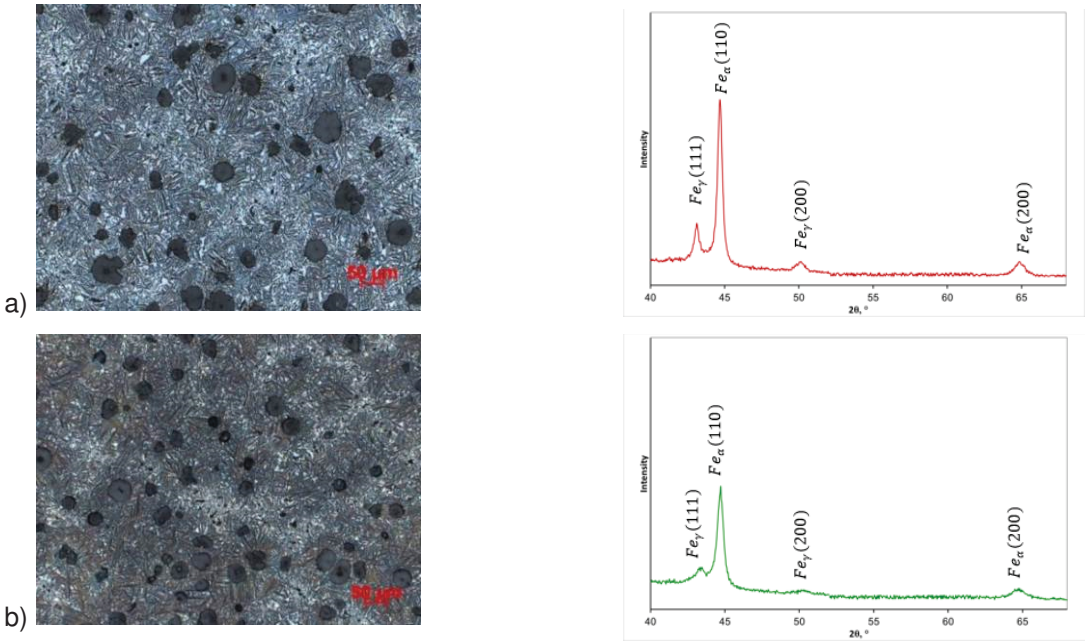

Figure 2 The representative microstructures and selected X-ray diffraction patterns of specimens austempered at two isothermal temperatures: a) W12 (T_{pi} = 400 °C, t_{pi} = 90 min, b) W8 (T_{pi} = 360 °C, t_{pi} = 120 min).

Table 3 gives the results of diffraction studies, which were used to determine the half-widths ($b_{1/2\gamma}$, $b_{1/2\alpha}$), and the calculated volume fractions of austenite (V_γ), carbon content in the retained austenite (C_γ), and the size of austenite and ferrite grains for individual variants of heat treatment.

Table 3 Parameters characterizing austenite and ferrite determined by the X-ray analysis for different isothermal temperatures

Variant	$T_{pi}, °C$	t_{pi}, min	$b_{1/2\gamma}, rad$	$b_{1/2\alpha}, rad$	$V_\gamma, \%$	$C_\gamma, \%$	D_γ, nm	D_α, nm
W12	400	90	0.55	0.55	24.3	2.0	26.8	18.3
W10	380	90	0.55	0.55	23.3	2.0	29.3	18.5
W8	360	90	0.50	0.55	18.9	2.1	32.2	18.8
W6	330	120	0.55	0.65	20.3	2.0	29.3	15.5
W4	300	120	0.70	0.70	12.8	2.0	23.0	14.8
W2	260	120	0.80	0.75	10.6	1.7	20.1	13.8

Changes in the austenite half-width values calculated for the upper and lower temperature range of isothermal transformation are shown in **Figure 2,** while changes in the size of the austenite and ferrite grains are shown in **Figures 3a** and **3b**, respectively.

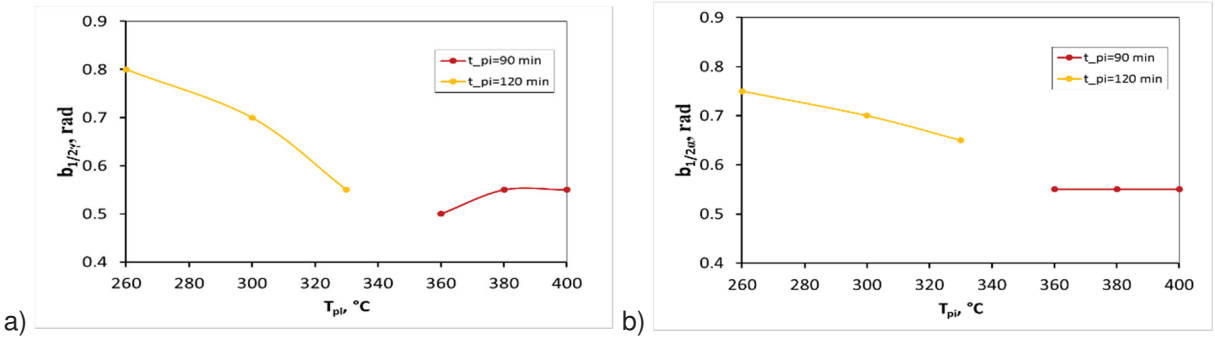

Figure 3 The effect of austempering temperature on the width of the diffraction line of: a) austenite, b) ferrite

As is apparent from **Figure 3**, for the lower range of ausferrite, the half-width of the diffraction line of austenite decreases with the increasing temperature of isothermal transformation. An opposite trend is observed in the range of upper ausferrite, which may be caused by the use of nickel as the only alloying addition promoting the half-width growth. Changes in the half-width of austenite in the range of upper ausferrite confirm an extension of the incubation period of the isothermal transformation. According to the literature data [12], the half-width may be reduced by either longer time or higher temperature of the isothermal transformation. The half-width of ferrite decreases with the increasing temperature of this transformation. This phenomenon is similar to the phenomenon observed during tempering of cast iron. The change indicates the decreasing degree of α phase supersaturation with carbon and drop in stress level. The stresses are caused by the heat treatment and also by the differences between volume fractions of austenite and ferrite after heat treatment.

The grain size of both austenite and ferrite is closely related to the temperature of isothermal transformation (**Figure 4**). In the range of lower ausferrite, the austenite grain size increases with the increasing temperature from 20.08 nm at 260 °C to 29.25 nm at 330 °C. In the range of upper ausferrite, the austenite grain size starts decreasing with the increasing temperature. This is associated with a proliferation of the side strips of ferrite, diminishing the size of austenite grains. The size of ferrite grains is nearly 1.5 times smaller than the size of austenite grains. The dimensional changes in the grains of ferrite, influenced by the temperature of isothermal transformation, are similar to the changes observed in austenite grains, though they are less intense and due in large part to the kinetics of transformations. The saturation of austenite with carbon results in ferrite decarbonizing.

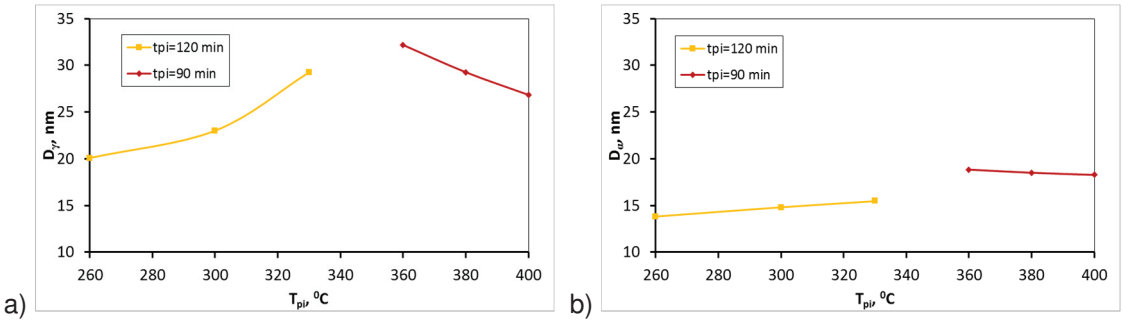

Figure 4 The effect of austempering temperature on the grain size of: a) austenite b) ferrite

The effect of austempering temperature on the volume fraction of austenite and carbon content in this austenite is shown in **Figures 5a** and **5b**, respectively.

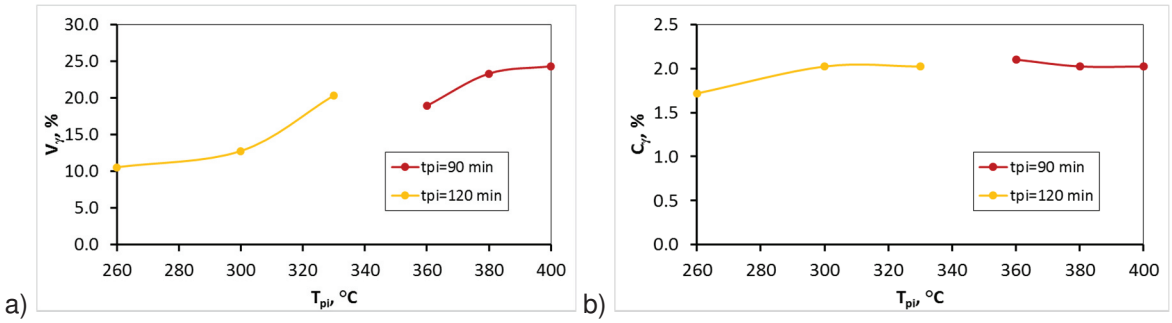

Figure 5 The effect of austempering temperature on: a) austenite volume fraction (V_{γ}), b) carbon content in austenite (C_{γ})

As is apparent from **Figure 5a**, with the increasing temperature of austempering, the austenite volume fraction is also increasing from 10.6 % at a temperature of 260℃ to 24.6 % at a temperature of 400 °C. **Figure 5b** shows changes of carbon content in the retained austenite calculated for the lower and upper temperature range of austempering. In the temperature range of 360 °C÷ 400 °C, the saturation of austenite with carbon reaches its maximum. Comparing the concentration of carbon in austenite it can be concluded that the higher is the temperature of isothermal transformation and the longer is the time of austempering, the higher is this content. However, the risk arising from the excessively long time of austempering may be the decomposition of carbon-saturated austenite to ferrite and carbide phase.

4. SUMMARY

The results of the X-ray phase analysis of ADI with the addition of Ni were presented. The literature gives practically no data on the results of such studies carried out for the cast iron. Therefore it is necessary to further explore the effect of Ni addition on the plastic properties of cast iron, such as the elongation and impact resistance, and also on the hardenability of heat-treated castings.

This paper discusses the effect of austempering temperature on the resulting volume fraction of austenite, carbon content in the austenite, and the size of austenite and ferrite grains. The presence of retained austenite in the matrix of ADI plays an important role in shaping of the ADI mechanical properties (mainly properties related with the alloy plastic behaviour, like elongation and impact strength). The study confirms that the volume fraction of the retained austenite is directly related to the temperature of isothermal transformation. With the increase of this temperature, the content of the retained austenite is also increasing (**Figure 4**). However, for a more complete verification of the applicability of the X-ray method in the phase evaluation of ADI matrix, alternative (microscopic) examinations supported by the computer image analysis should be

performed. Studies in this scope are in progress. The phenomena observed on metallographic samples and the mechanism of transformation kinetics should be verified on samples subjected to mechanical testing. The correlation of these results is expected to complement the nature of changes occurring during the austempering treatment of ADI.

ACKNOWLEDGEMENTS

Financial assistance of the NCN, project No. 2013/11/N/ST8/00326 is acknowledged.

REFERENCES

[1] ELLIOTTT R. Current status of austempered cast irons. Physical Metallurgy of Cast Iron V, 1994, vol. 4-5, pp. 1-16.

[2] AKBAY T., REED R., ATKINSON C. Modelling reaustenitization from ferrite/cementite mixtures in Fe-C steels. Acta Metall. Mater., 1994, vol. 47, no. 4, pp. 1469-1480.

[3] ZANARDI F. Machinable ADI (in Italy). AFS Transactions, 2005, 383 p.

[4] MRZYGŁÓD B., KOWALSKI A., OLEJARCZYK-WOŻEŃSKA I., ADRIAN H., GŁOWACKI M., OPALIŃSKI A. Effect of heat treatment parameters on the formation of ADI microstructure with additions of Ni, Cu, Mo. Archives of Metallurgy and Materials, 2015, vol. 60, no. 3A, pp.1941-1948.

[5] CETIN B., MECO H., ARSLAN E., UZUN M. C. Microstructural analysis of austempered ductile iron castings, Hittile Journal of Science and Engineering, 2016, vol. 3, no. 1, pp. 29-34.

[6] HUNG F. Y., CHEN L.H., LUI T.S. Phase transformation of an austempered duztile iron during an erosion process, Materials Transactions, 2004, vol. 45, no. 10, 2981-2986.

[7] UMALE S., LIKHITE A., PESHWE D. R., PATHAK S. U. Wear characteristic of low carbon equivalent austempered ductile iron (ADI), Indian Foundry Journal, 2014, vol. 60, no. 9, pp. 28-36.

[8] KUMARI U. R., RAO P. P. Study of wear behaviour of austempered ductile iron, Journal of Materials Science, 2009, vol. 44, no. 4, pp. 1082-1093.

[9] GIĘTKA T., DYMSKI S. The attempt at evaluation of the ADI microstructure with the use of the image analysis. Archives of Foundry Engineering, 2010, vol. 10, no. 2, pp. 57-62.

[10] KARP J. Rentgenowska ilościowa analiza fazowa RIAF austenitu w stalach. Hutnik, 1979, pp. 253-269.

[11] ŁAWRYNOWICZ Z., DYMSKI S. Carbon concentration of austenite in austempered ductile iron (ADI). Archives of Foundry Engineering, 2007, vol. 7, no. 3, pp. 93 - 98.

[12] ERIC O., BRDARIC T., STOJSAVLJEVIC N., MILAN T., GRAHOVAC N., DURICIC R. Determination of processing window for ADI, materials alloyed with copper. Metallurgical and Materials Engineering, 2010, vol. 16, no. 2, p.91-102.

[13] SENCZYK D. Rentgenowskie metody I techniki badania struktury materiałów. Poznań: Politechniki Poznańskiej, 1984, p. 259-281.

[14] CULLITY B.D. Elements of x-ray diffraction. Reading: Addison Wesley, 1974, p. 378-422.